New approach to the first-order phase transition of Lennard-Jones fluids

Chizuru Muguruma, Yuko Okamoto, and Masuhiro Mikami

Citation: J. Chem. Phys. **120**, 7557 (2004); doi: 10.1063/1.1687682
View online: https://doi.org/10.1063/1.1687682
View Table of Contents: http://aip.scitation.org/toc/jcp/120/16
Published by the American Institute of Physics

New approach to the first-order phase transition of Lennard-Jones fluids

Chizuru Muguruma[a)]
Faculty of Liberal Arts, Chukyo University, Toyota, Aichi 470-0393, Japan

Yuko Okamoto
Department of Theoretical Studies, Institute for Molecular Science, Okazaki, Aichi 444-8585, Japan and Department of Functional Molecular Science, The Graduated University for Advanced Studies, Okazaki, Aichi 444-8585, Japan

Masuhiro Mikami
Research Institute for Computational Sciences, National Institute of Advanced Industrial Science and Technology, Tsukuba, Ibaraki 305-8568, Japan

(Received 27 October 2003; accepted 27 January 2004)

The multicanonical Monte Carlo method is applied to a bulk Lennard-Jones fluid system to investigate the liquid–solid phase transition. We take the example of a system of 108 argon particles. The multicanonical weight factor we determined turned out to be reliable for the energy range between −7.0 and −4.0 kJ/mol, which corresponds to the temperature range between 60 and 250 K. The expectation values of the thermodynamic quantities obtained from the multicanonical production run by the reweighting techniques exhibit the characteristics of first-order phase transitions between liquid and solid states around 150 K. The present study reveals that the multicanonical algorithm is particularly suitable for analyzing the transition state of the first-order phase transition in detail. © *2004 American Institute of Physics.* [DOI: 10.1063/1.1687682]

I. INTRODUCTION

The great advancement of computer technology and simulation technique has made computer simulation an effective tool in many fields of chemistry and physics. However, simulations of complex systems with many degrees of freedom, such as spin glasses and biopolymers, are still greatly hampered by the multiple-minima problem. This is because conventional canonical simulations at low temperatures tend to get trapped in one of a large number of local-minimum states on the potential energy surface.

The multicanonical (MUCA) algorithm[1,2] has been introduced as one of the methods to overcome this multiple-minima problem and has been applied to study first-order phase transitions[1–14] (for recent reviews, see Refs. 15 and 16). The algorithm is based on an artificial non-Boltzmann weight factor and performs a free one-dimensional random walk in potential energy space, which allows the simulation to avoid getting trapped in states of energy local minima. Moreover, one can calculate the expectation values of thermodynamic quantities as functions of temperature by applying the single-histogram reweighting techniques[17] to the results of one long production run.

A Lennard-Jones fluid system, such as an argon fluid, is one of the typical systems with first-order phase transitions.[7,10,18] It has been known that solid argon can be easily-obtained by simulated annealing.[19] However, it is very difficult to obtain thermodynamic quantities around the phase transition point by such optimization methods, because the process of cooling breaks thermal equilibrium. The MUCA Monte Carlo (MUCAMC) method always maintains the thermal equilibrium and is particularly suitable for investigating phase transitions. In the present study, we apply the MUCAMC method to the bulk argon system and investigate the changes in thermodynamic quantities across the phase transition point.

This article is organized as follows: In Sec. II, the MUCAMC method is briefly described. We report the results of the MUCAMC simulation of a bulk argon system in Sec. III. Conclusions follow in Sec. IV.

II. COMPUTATIONAL METHODS

A. Multicanonical ensemble

Although the MUCA algorithm is explained in detail elsewhere,[14–16] we give a short overview in this subsection for completeness. In the canonical ensemble, the probability distribution of the potential energy E, $P_B(E;T)$, is given by the product of the density of states $n(E)$ and the Boltzmann weight factor $W_B(E;T)$:

$$P_B(E;T) \propto n(E) W_B(E;T) = n(E) e^{-\beta E}, \tag{1}$$

where β is the inverse temperature $1/k_B T$ with the Boltzmann constant k_B and temperature T. Because $n(E)$ is a rapidly increasing function and $W_B(E;T)$ decreases exponentially, $P_B(E;T)$ generally has a bell-like shape.

In MUCA ensemble each state is weighted by a non-Boltzmann weight factor $W_{\mathrm{mu}}(E)$, which we refer to as the MUCA weight factor, so that a uniform potential energy distribution may be obtained:

$$P_{mu}(E) \propto n(E) W_{\mathrm{mu}}(E) \equiv \text{constant}. \tag{2}$$

The flat artificial energy distribution implies that a one-dimensional free random walk in the potential energy space

a)Electronic mail: muguruma@lets.chukyo-u.ac.jp

is realized. The random walk allows the system to escape from any local-minimum-energy states and to sample the configurational space much more widely with a smaller number of simulation steps than the conventional canonical Monte Carlo (MC) or molecular dynamics methods.

From the definition in Eq. (2), the MUCA weight factor $W_{\mathrm{mu}}(E)$ is inversely proportional to the density of the states $n(E)$ and can be written as follows:

$$W_{\mathrm{mu}}(E) \equiv e^{-S(E)/k_B} = \frac{1}{n(E)}, \tag{3}$$

where $S(E)$ is the entropy in the microcanonical ensemble:

$$S(E) = k_B \ln n(E). \tag{4}$$

Since the density of states of the system is usually unknown, the MUCA weight has to be determined numerically by iterations of short preliminary runs. In the present study, we employ the iterative procedure in Ref. 20.

A MUCAMC simulation is performed, for instance, with the usual Metropolis criterion:[21] The transition probability of state x with potential energy E to state x' with potential energy E' is given by

$$w(x \to x') = \begin{cases} 1, & \text{for } \Delta S \leqslant 0, \\ \exp(-\Delta S/k_B), & \text{for } \Delta S > 0, \end{cases} \tag{5}$$

where

$$\Delta S \equiv S(E') - S(E). \tag{6}$$

Once the MUCA weight factor [equivalently the entropy $S(E)$] is given, one performs a long MUCA production run. By tracing the potential energy surface during the simulation, the global-minimum-energy state can be identified. Moreover, adopting the reweighting techniques, the expectation value of a physical quantity A at any temperature T $(=1/k_B\beta)$ is given by

$$\langle A \rangle_T = \frac{\sum_E A(E) n(E) e^{-\beta E}}{\sum_E n(E) e^{-\beta E}}, \tag{7}$$

where the optimal density of states $n(E)$ is obtained by the single-histogram reweighting techniques [see Eq. (2)]:[17]

$$n(E) = \frac{H_{\mathrm{mu}}(E)}{W_{\mathrm{mu}}(E)}, \tag{8}$$

and $H_{\mathrm{mu}}(E)$ is the recorded histogram of the probability distribution of potential energy $P_{\mathrm{mu}}(E)$ in the production run.

To obtain a more accurate weight function, we repeat M-independent MUCAMC simulations. The best estimate of the density of states $n(E)$ is determined by the multiple-histogram reweighting techniques:[22,23]

$$n(E) = \frac{\sum_{m=1}^{M} H_m(E)}{\sum_{m=1}^{M} n_m e^{g_m - S_m(E)/k_B}}, \tag{9}$$

where

$$e^{-g_m} = \sum_E n(E) e^{-S_m(E)/k_B}. \tag{10}$$

Here, $H_m(E)$, $S_m(E)$, and n_m are, respectively, the potential energy histogram, the entropy, and the total number of samples of the mth MUCAMC production run $(m = 1,...,M)$. Note that Eqs. (9) and (10) are solved self-consistently by iteration.

B. Computational details

We put 108 argon particles in a cubic cell with periodic boundary conditions. The edge size is fixed at 16.314 Å so that the density of the system is 1.65 g/cm^3, which corresponds to the density of solid argon at 40.15 K. A pair of argon particles with distance r_{ij} interacts through the Lennard-Jones pair potential

$$v(r_{ij}) = 4\varepsilon \left[\left(\frac{\sigma}{r_{ij}} \right)^{12} - \left(\frac{\sigma}{r_{ij}} \right)^{6} \right], \tag{11}$$

where the potential parameters of argon are $\varepsilon = 0.9961$ kJ/mol and $\sigma = 3.405$ Å,[24] and the total potential energy of the system that consists of N argon particles is given by

$$E = \sum_{i=1}^{N-1} \sum_{j>i}^{N} v(r_{ij}). \tag{12}$$

The interactions of all particles are truncated at a distance of 8.157 Å which corresponds to a half length of the edge size. The MUCA weight factor was determined for the temperature range $T \leqslant 250$ K. The conventional canonical MC simulations were also carried out at $T = 60$ and 250 K for comparison with the MUCAMC simulation. Thermodynamic quantities are calculated by the reweighting techniques in Eqs. (7) and (8). For instance, the pressure P and heat capacity C_V are calculated from the following equations:

$$P = \frac{N k_B T}{V} + \frac{1}{3V} \sum_{i=1}^{N-1} \sum_{j>i}^{N} r_{ij} f_{ij}, \tag{13}$$

$$C_V = \frac{\langle E^2 \rangle_T - \langle E \rangle_T^2}{k_B T^2}, \tag{14}$$

where f_{ij} is the pair force acting on atom i due to atom j and V is the volume of the system.

One MC sweep is defined to consist of 108 coordinate updates of a randomly chosen particle with the Metropolis evaluation for each update. All calculations were performed with our own computer code.

III. RESULTS AND DISCUSSION

A. Multicanonical weight factor determination

The uniformity of the probability distribution depends on the accuracy of the multicanonical weight factor. It is difficult to obtain the optimal multicanonical weight factor by one simulation. Therefore, the weight factor was determined by the following four steps. First, we selected four different tentative weight factors and performed a MUCAMC simulation of 10^7 MC sweeps with each weight

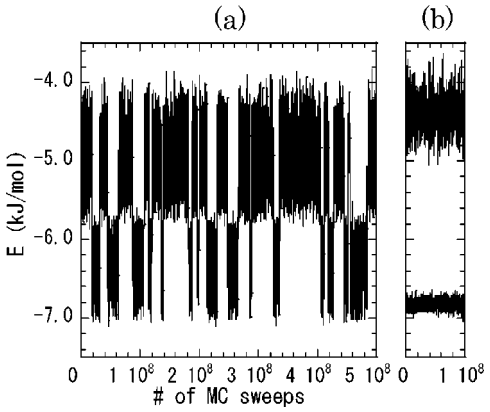

FIG. 1. Time series of total potential energy obtained by (a) a long production run of the MUCAMC simulation and (b) the conventional canonical MC calculations at temperatures 60 and 250 K.

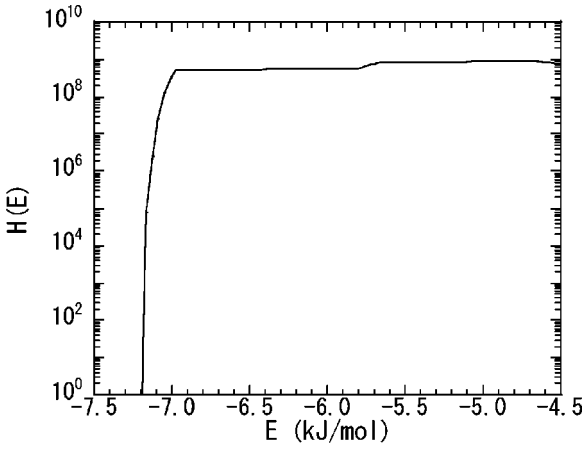

FIG. 2. Histogram of the total potential energy distribution that was obtained by the MUCAMC production run.

factor to obtain histograms. Second, the multiple-histogram reweighting techniques of Eqs. (9) and (10) were applied to obtain a better MUCA weight factor. Third, a MUCAMC simulation of 5×10^8 MC sweeps was performed to further refine the weight factor around the phase transition point. Here, the energy region of the simulation was restricted between -6.5 and -5.0 kJ/mol by extrapolating the entropy $S(E)$ in Eq. (3) linearly outside this energy range. Finally, the best estimate of the MUCA weight factor was obtained by the single-histogram reweighting techniques [see Eqs. (3) and (8)]. We then perform the MUCAMC production run of 5×10^8 MC sweeps to calculate various thermodynamic quantities.

The ''time series'' of total potential energy from the MUCAMC production run is shown in Fig. 1(a). We indeed see a random walk between -7.0 and -4.0 kJ/mol. The energy region is divided into two parts around -5.75 kJ/mol, and the transition between these two regions takes place 15 times during the production run. The time series of the total potential energy obtained by the conventional canonical MC simulations with 10^8 MC sweeps at temperatures 60 and 250 K are also shown in Fig. 1(b). Comparing Figs. 1(a) and 1(b), we find that the MUCAMC simulation of Fig. 1(a) covers the energy range corresponding to the temperature range between 60 and 250 K.

Figure 2 is the histogram of the potential energy distribution that was obtained by the MUCAMC production run. We observe a flat histogram in the energy region between -7.0 and -4.5 kJ/mol. This implies that the multicanonical ensemble is realized in this energy region. We can calculate entropy $S(E)=k_B\ln n(E)$ from the result of the MUCAMC production run by the single-histogram reweighting techniques in Eq. (8). The entropy thus calculated is shown in Fig. 3.

Snapshots obtained from the MUCAMC production run are shown in Fig. 4. In the higher-energy state of Fig. 4(a), argon particles are scattered randomly, whereas argon particles are almost regularly arranged in the lower-energy state of Fig. 4(b). Therefore, we consider that the high-energy state corresponds to the liquid state and the low-energy state to the solid state. The lowest-energy structure obtained during this MUCAMC simulation is shown in Fig. 4(c). A higher regularity is indeed observed in Fig. 4(c).

B. Analyses of the multicanonical Monte Carlo production run

The results of the MUCAMC production run are analyzed by applying the reweighting techniques. Figure 5 shows the canonical probability distributions at $T=130$, 140, 150, 160, and 170 K. There is a clear two-peak distribution around $T=150$ K, suggesting the existence of a first-order phase transition. The boundary of two peaks lies around -5.75 kJ/mol. We remark that this boundary is also recognized in the histogram of Fig. 2 and the entropy of Fig. 3. The canonical probability distribution has a single peak of solid state at 130 K. As the temperature becomes higher, the signal of liquid state is stronger and that of solid state is weaker. At 170 K, the canonical probability distribution has a single peak of liquid state. Two peaks exist and have almost equal heights at 150 K. This means that the liquid and solid states coexist in the system at 150 K and the temperature is very close to the phase transition point.

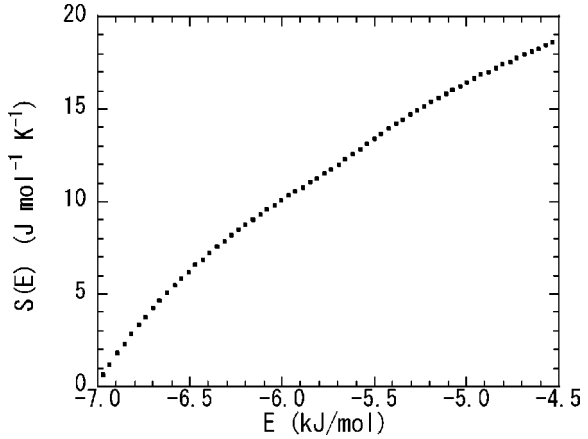

FIG. 3. The entropy as a function of total potential energy obtained by the MUCAMC production run. We have set the value of entropy to zero at $E=-7.0$ (kJ/mol).

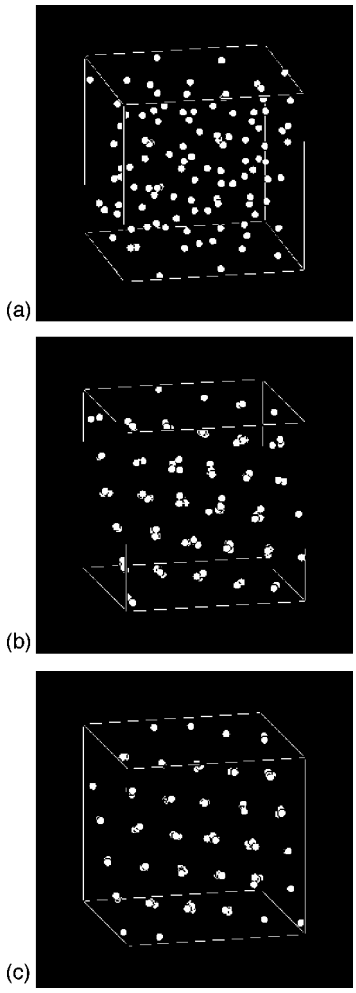

FIG. 4. Snapshots obtained by the MUCAMC production run. The total potential energy is (a) −5.04, (b) −6.47, and (c) −7.18 kJ/mol, respectively. Pictures are the projection along a crystal axis. The mass of argon particles are observed in the snapshots (b) and (c) because of the fluctuation.

"Potential of mean force" as a function of energy can be calculated by $F=-k_BT\ln P_B(E;T)$ from the canonical probability distribution $P_B(E;T)$ in Fig. 5. This potential of mean force at the corresponding temperatures is shown in Fig. 6. Near the transition temperature, a double-well-like profile is observed. The well depth of the two states is almost equivalent at 150 K and the free energy barrier height between the two states is about 2 kJ/mol at this transition point.

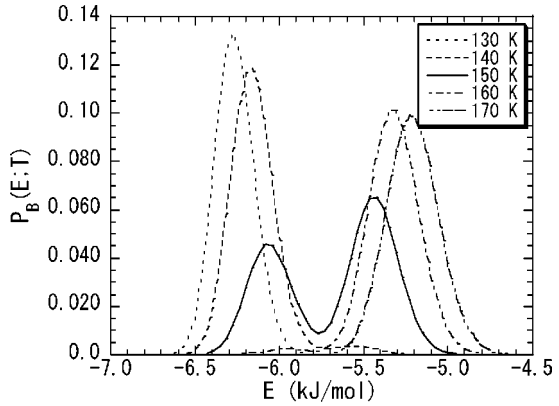

FIG. 5. The canonical probability distributions at $T=130$, 140, 150, 160, and 170 K, which were obtained from the MUCAMC production run by the reweighting techniques.

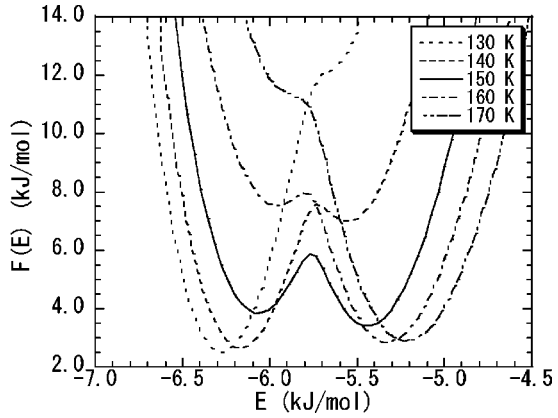

FIG. 6. Potential of mean forces obtained from the canonical probability distributions at $T=130$, 140, 150, 160, and 170 K.

C. Thermodynamic quantities

We are interested in the change in the physical quantities by the phase transition. We calculated the expectation values of thermodynamic quantities at every 5 K from 50 to 250 K. Average energy, pressure, heat capacity, entropy, and Helmholtz free energy are shown in Fig. 7, which are obtained by the MUCAMC production run by applying the reweighting techniques in Eqs. (7) and (8).

The average total potential energy is shown in Fig. 7(a). As we have already shown in Fig. 1, the average total potential energy shows that the energy range from −7.0 to −4.5 kJ/mol corresponds to the temperature range from 60 to 250 K. The discontinuous change in the average energy implies that the phase transition point is 150 K. The change in energy at the phase transition point is from −6.2 to −5.4 kJ/mol, which amount to 0.8 kJ/mol. The pressure, shown in Fig. 7(b), also shows discontinuous change from 0.22 to 0.48 GPa at 150 K, which agrees well with the experimental fact that the melting point is around 150 K under the corresponding pressure.[25]

Heat capacity is shown in Fig. 7(c). A significant peak at 150 K means that energy which the system receives is used for the phase transition rather than for rising the temperature around the phase transition point. This again implies the existence of a phase transition at this temperature. The width of the peak is 25 K, which is rather wide. We expect that it would become narrower as the system size becomes larger.

Calculating entropy by the ordinary molecular simulation methods requires a lot of efforts. However, entropy $S(E)$ can be easily obtained by the MUCA algorithm. The entropy in the canonical ensemble at temperature T is calculated by the reweighting techniques as follows:

$$S(T)=\frac{\sum_E S(E)n(E)e^{-\beta E}}{\sum_E n(E)e^{-\beta E}}, \tag{15}$$

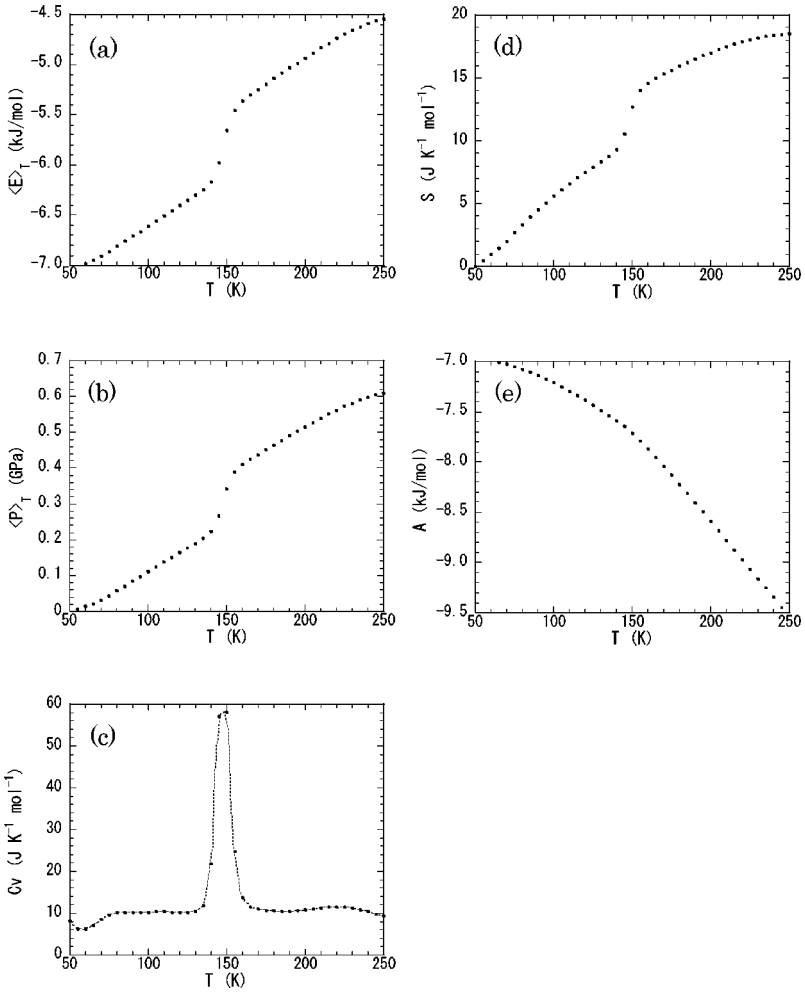

FIG. 7. The expectation values of the thermodynamic properties: (a) Total potential energy, (b) pressure, (c) heat capacity, (d) entropy, and (e) Helmholtz free energy obtained from the MUCAMC production run by the reweighting techniques. The expectation values were calculated at each 5 K from 50 to 250 K.

and is shown in Fig. 7(d). The discontinuous change in slope is again recognized for the entropy. The change in the entropy at the phase transition point is 5 $\mathrm{J\,K^{-1}\,mol^{-1}}$. We remark that the differences in energy and in entropy at the phase transition point satisfy the thermodynamic relation $\Delta S = \Delta E/T$.

Helmholtz free energy is also one of the physical quantities that are difficult to calculate by the ordinary computer simulation methods. In the MUCA algorithm, we can calculate the Helmholtz free energy by the relation $A(T) = \langle E \rangle_T - TS(T)$. It is shown in Fig. 7(e) and the change in the slope is again observed at 150 K. All these changes at 150 K are characteristics of the first-order phase transition.

D. Radial distribution function

The radial distribution functions (RDFs) were also calculated at $T = 100$, 130, 140, 150, 160, and 170 K by the reweighting techniques from the MUCAMC production run. The resulting RDFs are shown in Fig. 8. The RDFs at 100 and 130 K are almost identical with that at 140 K. We can observe four peaks at 3.8, 5.4, 6.6, and 7.6 Å in the RDF at 100 K, which is the shortest distance between argon particles, $\sqrt{2}$ times, $\sqrt{3}$ times, and twice the shortest distance, which is the feature of the face-centered-cubic crystal. The RDF at 160 K is also almost identical with that at 170 K. Weak peaks at 5.4 and 7.6 Å completely disappeared and broader peaks are observed at 3.6 and 6.8 Å. This implies that the regular crystal structure of argon particles at lower temperature is changed into the structure that has less regularity of the liquid state as the temperature rises. The RDF at 150 K has intermediate characteristics between those of liquid and solid states. This suggests that both liquid and solid state structures coexist at 150 K and the average of these two states appear in the RDF.

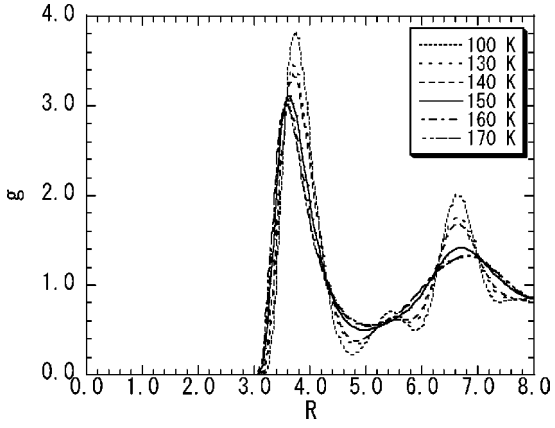

FIG. 8. The argon–argon radial distribution function g at $T = 100$, 130, 140, 150, 160, and 170 K, which were obtained from the MUCAMC production run by the reweighting techniques.

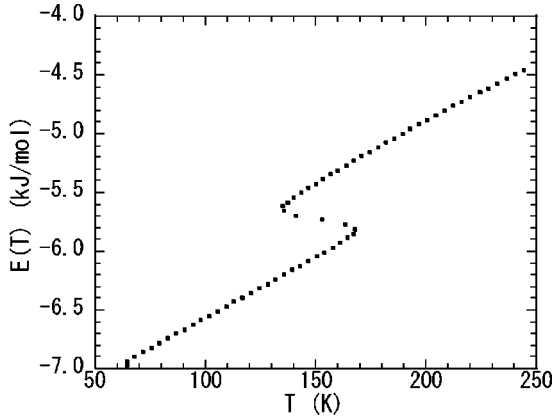

FIG. 9. Change in total potential energy calculated by the multicanonical weight factor.

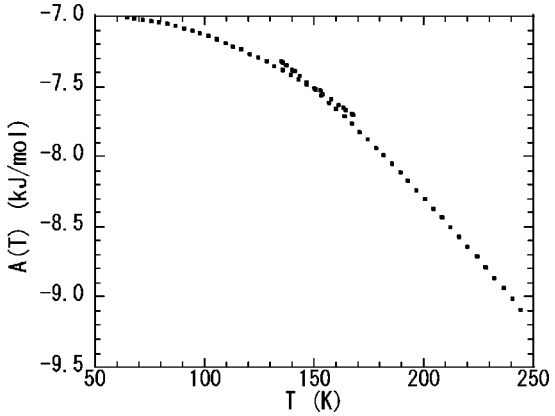

FIG. 11. Helmholtz free energy estimated by $E(T)-TS(T)$, where $E(T)$ is total potential energy in Fig. 9, T is temperature and $S(T)$ is multicanonical entropy in Fig. 10.

E. Analysis of transition state

The MUCA weight factor is a function of entropy. Thus, by using the relation

$$\frac{\partial S(E)}{\partial E}=\frac{1}{T}, \tag{16}$$

temperature can be expressed as a function of energy. Figure 9 shows the relation between the total potential energy and temperature. Although we have seen a discontinuous change in average energy at 150 K [see Fig. 7(a)], we see a continuous sigmoidal change around the phase transition point in Fig. 9. The three energy states observed near 150 K correspond to the three stationary points in the potential of mean force of Fig. 6, and the middle one is not a stable state but a transition state between solid and liquid states.

The relation between energy and temperature in Eq. (16) can be used to express entropy as a function of temperature and it is shown in Fig. 10. The entropy also shows the continuous sigmoidal change around the phase transition point. These results imply that when the system is cooled from the liquid state, it undergoes a supercooled state and then an overheated state during the phase transition.

Helmholtz free energy is estimated by $A(T)=E(T)-TS(T)$. The result is shown in Fig. 11, where $E(T)$ in Fig. 9 and $S(T)$ in Fig. 10 are used. The behavior of this free energy implies that the liquid state is supercooled until 130 K, shifted to the overheated solid state until 170 K via an unstable transition state, and finally undergoes the phase transition to the solid state. The phase transition takes place when free energy of solid state coincides with that of liquid state.

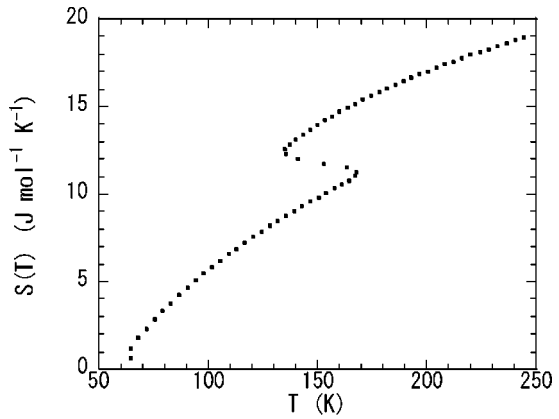

FIG. 10. Change in multicanonical entropy calculated by the multicanonical weight factor.

These results suggest that the MUCAMC method has an additional feature for the study of first-order phase transition in the sense that we can study transition states in detail (for a variant of MUCA algorithm that allows efficient sampling around transition states, see also Ref. 26). The study of transition states is usually very difficult with the ordinary canonical simulation method, because these states are rarely observed in such simulations. The MUCAMC method yields many transitions between two states during the simulation (see the histogram in Fig. 2). The potential of the mean force in Fig. 6 suggests that transitions occur in the energy region between -5.7 and -5.8 kJ/mol. Snapshots of some of the configurations within the transition energy region are shown in Fig. 12. The configuration in Fig. 12(a) is close to the liquid state, that in Fig. 12(c) is much close to the solid state, and that in Fig. 12(b) is the mixture of the liquid and solid states. In particular, the upper half of Fig. 12(b) roughly corresponds to the solid state and the lower-half to the liquid state. The configuration of Fig. 12(b) should be close to the configuration at the phase transition point.

IV. CONCLUDING REMARKS

The MUCAMC method was applied to the bulk argon system. Comparing the energy ranges covered by the conventional canonical MC simulations at 60 and 250 K with the histogram of energy distribution obtained from the MUCA production run, we found that the MUCA weight factor that we determined was reliable for the energy range between -7.0 and -4.5 kJ/mol, which corresponds to the temperature range from 60 to 250 K. The physical quantities,

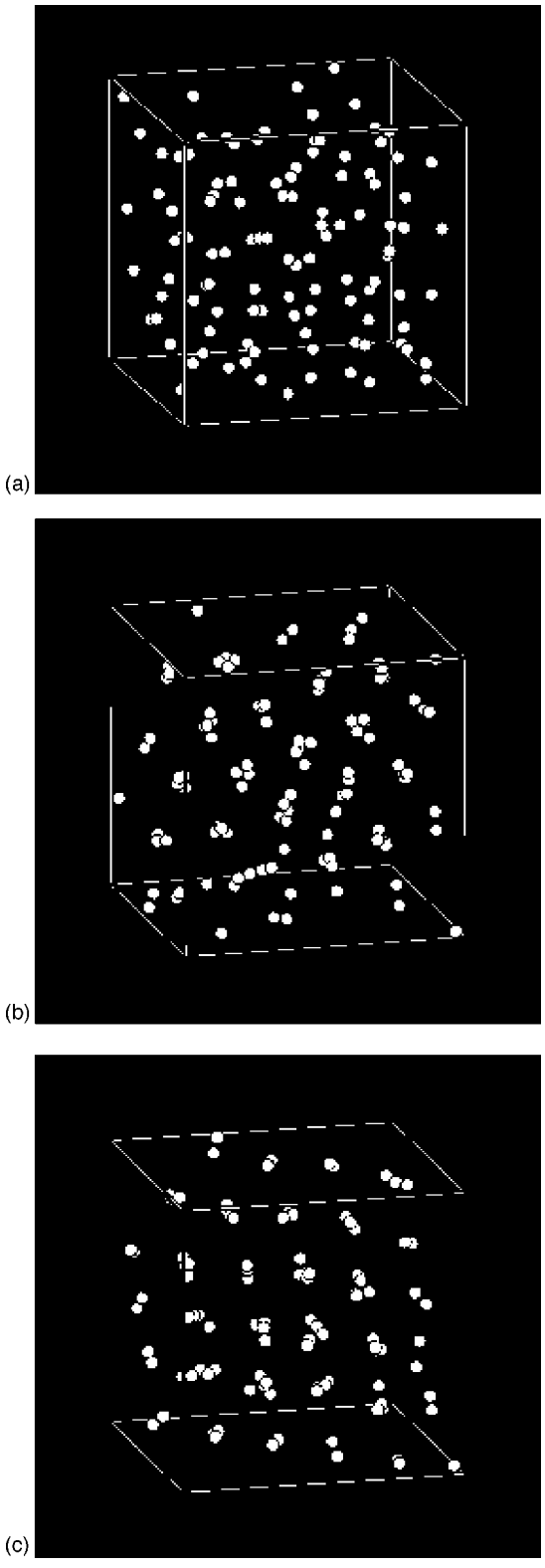

FIG. 12. Snapshots of the configurations whose energies are in the transition-state region, which are obtained by the MUCAMC production run. The total potential energy is (a) −5.74, (b) −5.77, and (c) −5.75 kJ/mol, respectively. Pictures are the projection along a crystal axis. The fluctuation of argon particles are observed in the snapshots (b) and (c).

snapshots, and radial distribution functions showed that the first-order phase transition between the liquid and solid states is observed around 150 K. The analyses of the MUCA weight factor revealed that the liquid–solid phase transition takes place through both the supercooled condition of liquid state and overheated condition of the solid state. In the present study, a configuration that coexists in both the liquid and solid states is found as one of the transition-state structures around the transition point.

The MUCAMC method has the following features: (1) The global-minimum structure is identified, and (2) the expectation values of a physical quantity at any temperature can be calculated by the reweighting techniques. In the present study, we found an additional feature that (3) the MUCAMC method is particularly suitable for analyzing the transition state of the first-order phase transition in detail. We are further investigating the feature of the transition states as a future work. Though we think the finite-size effects do not cause significant differences, we are also investigating these effects by using bigger systems.

ACKNOWLEDGMENTS

Some of the calculations were performed at the Research Center for Computational Science at the Okazaki National Research Institute and the Tsukuba Advanced Computing Center at the National Institute of Advanced Industrial Science and Technology. The present study is supported in part by the grant from the Hori Information Science Promotion Foundation, Chukyo University, and the Joint Study program of the Institute for Molecular Science. One of the authors (C.M.) thanks Professor B. A. Berg and Professor U. H. E. Hansmann for fruitful discussions.

[1] B. A. Berg and T. Neuhaus, Phys. Lett. B **267**, 249 (1991).
[2] B. A. Berg and T. Neuhaus, Phys. Rev. Lett. **68**, 9 (1992).
[3] B. A. Berg and T. Celik, Phys. Rev. Lett. **69**, 2292 (1992).
[4] U. H. E. Hansmann and Y. Okamoto, J. Comput. Chem. **14**, 1333 (1993).
[5] Y. Okamoto and U. H. E. Hansmann, J. Phys. Chem. **99**, 11276 (1995).
[6] W. Janke and S. Kappler, Phys. Rev. Lett. **74**, 212 (1995).
[7] N. B. Wilding, Phys. Rev. E **52**, 602 (1995).
[8] B. A. Berg and W. Janke, Phys. Rev. Lett. **80**, 4771 (1998).
[9] K. K. Bhattacharya and J. P. Sethna, Phys. Rev. E **57**, 2553 (1998).
[10] H. Liang and H. Chen, J. Chem. Phys. **113**, 4469 (2000).
[11] C. Muguruma, Y. Okamoto, and M. Mikami, Internet Electron. J. Mol. Des. **1**, 583 (2002).
[12] B. A. Berg, Comput. Phys. Commun. **247**, 52 (2002).
[13] E. Bittner, W. Janke, and D. B. Saakian, Phys. Rev. E **67**, 016105 (2003).
[14] B. A. Berg, Comput. Phys. Commun. **153**, 397 (2003).
[15] B. A. Berg, Fields Institute Communications **26**, 1 (2000); cond-mat/99009236.
[16] A. Mitsutake, Y. Sugita, and Y. Okamoto, Biopolymers **60**, 96 (2001).
[17] A. M. Ferrenberg and R. H. Swendsen, Phys. Rev. Lett. **61**, 2635 (1988); *ibid.* **63**, 1658 (1989).
[18] A. Rytkönen, S. Valkealahti, and M. Manninen, J. Chem. Phys. **108**, 5826 (1998).
[19] S. Kirkpatrick, C. D. Gelatt, Jr., and M. P. Vecchi, Science **220**, 671 (1983).
[20] B. A. Berg, Nucl. Phys. B (Proc. Suppl.) **63A–C**, 982 (1998).
[21] N. Metropolis, A. W. Rosenbluth, M. N. Rosenbluth, A. H. Teller, and E. Teller, J. Chem. Phys. **21**, 1087 (1953).
[22] A. M. Ferrenberg and R. H. Swendsen, Phys. Rev. Lett. **63**, 1195 (1989).
[23] S. Kumar, D. Bouzida, R. H. Swenden, P. A. Kollmann, and J. M. Rosenberg, J. Comput. Chem. **13**, 1011 (1992).
[24] G. C. Maitland, M. Rigby, E. B. Smith, and W. A. Wakeham, *Intermolecular Forces: their Origin and Determination* (Clarendon, Oxford, 1981).
[25] F. Datchi, P. Loubeyre, and R. LeToullec, Phys. Rev. B **61**, 6535 (2000).
[26] B. A. Berg, H. Noguchi, and Y. Okamoto, Phys. Rev. E **68**, 036126 (2003).